

Ultrafast Doublon Dynamics in Photoexcited $1T$ -TaS₂

M. Ligges,^{1,*} I. Avigo,¹ D. Golež,² H. U. R. Strand,² Y. Beyazit,¹ K. Hanff,³ F. Diekmann,³ L. Stojchevska,¹
M. Kalläne,³ P. Zhou,¹ K. Rossnagel,³ M. Eckstein,⁴ P. Werner,² and U. Bovensiepen¹

¹*Faculty of Physics, University of Duisburg-Essen, 47048 Duisburg, Germany*

²*Department of Physics, University of Fribourg, 1700 Fribourg, Switzerland*

³*Institute of Experimental and Applied Physics, University of Kiel, 24098 Kiel, Germany*

⁴*Max Planck Research Department for Structural Dynamics, University of Hamburg-CFEL, 22761 Hamburg, Germany*



(Received 14 February 2017; revised manuscript received 28 December 2017; published 18 April 2018)

Strongly correlated materials exhibit intriguing properties caused by intertwined microscopic interactions that are hard to disentangle in equilibrium. Employing nonequilibrium time-resolved photoemission spectroscopy on the quasi-two-dimensional transition-metal dichalcogenide $1T$ -TaS₂, we identify a spectroscopic signature of doubly occupied sites (doublons) that reflects fundamental Mott physics. Doublon-hole recombination is estimated to occur on timescales of electronic hopping $\hbar/J \approx 14$ fs. Despite strong electron-phonon coupling, the dynamics can be explained by purely electronic effects captured by the single-band Hubbard model under the assumption of weak hole doping, in agreement with our static sample characterization. This sensitive interplay of static doping and vicinity to the metal-insulator transition suggests a way to modify doublon relaxation on the few-femtosecond timescale.

DOI: [10.1103/PhysRevLett.120.166401](https://doi.org/10.1103/PhysRevLett.120.166401)

Complex matter is characterized by strong interactions between different microscopic degrees of freedom, often resulting in rich phase diagrams where tiny variations of controllable parameters can lead to significant changes of the macroscopic material properties [1]. This competition or coexistence often occurs on comparable energy scales, and thus is only partly accessible in the spectral domain. The dynamics of such systems, driven out of equilibrium by an external stimulus, can shed new light on the underlying short- and long-range interactions because different coupling mechanisms result in dynamics on experimentally distinguishable femto- to picosecond timescales [2]. In contrast to materials with well-defined quasiparticles, the theoretical description and analysis of nonequilibrium phenomena in strongly correlated electron systems is challenging [3]. Model studies have predicted intriguing effects of electron-phonon coupling [4–6], spin excitations [7–9], and dynamical screening [10], but connecting these insights to measurements on real materials has rarely been attempted. In this Letter, we analyze the photoinduced electron dynamics in a quasi-two-dimensional system with strong electron-electron and electron-phonon interaction and a finite density of defects. Our combined theoretical and experimental study shows how to disentangle such competing processes in the time domain, and how the nature of photoexcited carriers and the dominant relaxation pathways can be identified.

$1T$ -TaS₂ is a layered crystal that exhibits a manifold of electronically and structurally ordered phases [11–13], recently amended by quantum spin liquid properties [14]. In its high-temperature state ($T > 542$ K), the system is

undistorted and metallic, while cooling results in the formation of various charge density waves (CDW) with an increasing degree of commensurability and a transition to semiconductorlike behavior. Below the critical temperature of 180 K, a commensurate periodic lattice distortion is formed, giving rise to the formation of “David star”-shaped 13-Ta-atom cluster sites. This structural distortion is accompanied by a rearrangement of the partially filled Ta $5d$ band into submanifolds. The uppermost half-filled band is prone to a Mott-Hubbard transition, forming an occupied lower Hubbard band (LHB) representing a single particle population per cluster and an unoccupied upper Hubbard band (UHB) indicating a double population of cluster sites. On-site Coulomb interaction acts on these doublons and leads to an energy gap of 350–420 meV between the LHB and UHB [15]. This widely accepted picture was recently challenged [16]. It was proposed that the formation of an energy gap can be explained by orbital texturing, which implies that Mott physics is not primarily responsible for the insulating state. Our combined theoretical and experimental effort shows how such ambiguity can be addressed under nonequilibrium conditions. We identify a hierarchy of timescales which allows for specific studies of electronic correlation effects in complex materials.

Time- and angle-resolved photoemission spectroscopy is a powerful tool for exploring the ultrafast electronic response of $1T$ -TaS₂ on femto- to picosecond timescales [17–20]. Our present studies were carried out in a pump-probe scheme in normal emission geometry (which probes electronic states at the center of the Brillouin zone) on *in situ* cleaved single crystals, which exhibit nonperfect stoichiometric ratios

($1T\text{-Ta}_{(1-x)}\text{S}_2$ with $x \leq 0.03$) [21] (see Supplemental Material for sample characterization [22]). The samples were excited with 50 fs laser pulses from a regenerative Ti:Sa laser amplifier ($\hbar\omega_{\text{pump}} = 1.55$ eV) operating at a 250 kHz repetition rate and probed by direct photoemission using frequency-quadrupled pulses ($\hbar\omega_{\text{probe}} = 6.2$ eV). The pump-probe cross-correlation width was determined to be 110 ± 5 fs (Gaussian full width at half maximum) through the fastest observed response, and the corresponding maximum was set as time zero. The spectral resolution of 80 meV was determined by analyzing the width of the high-temperature Fermi edge (assumed to be rigid). Incident excitation fluences F were kept well below the critical energy density necessary to drive the system thermally into the nearly commensurate CDW phase [23].

We present data obtained in a weak excitation limit and at a base temperature of $T = 30$ K, a situation in which we expect only minor modifications of the CDW-ordered state. Assuming that every absorbed pump photon excites one valence electron on one cluster site once, the excited electron density in the first atomic layers is estimated to be $< 3\%$ for $F = 100 \mu\text{J}/\text{cm}^2$ [24]. Under such conditions, we observe a photoemission peak at $E - E_F \approx 175$ meV [Fig. 1(a)] that is barely visible for higher F and T , even when the transient spectra are averaged over the relevant delay range, as displayed in Figs. 1(b) and 1(c). The contrast between this photoemission peak and the

underlying background differs between samples of different growth batches, a finding that we assign to minute variations of stoichiometric composition, and thus, hole doping (see Supplemental Material for details [22]). The general behavior, however, is the same for all samples under investigation. Figure 1(a) shows a false-color representation of time-dependent photoemission spectra. Upon pumping, a broad excitation continuum is generated that reaches up to $E - E_F \approx 1.5$ eV. The population decay of this continuum is resolved, and the closer to E_F the intensity is analyzed, the longer the relaxation times become—a behavior well known for electronic excitations at metal surfaces [27]. In contrast, the sharp spectral signature at 175 meV responds significantly faster. Due to its femtosecond dynamics, we interpret this feature as the UHB that directly reflects double occupation of cluster sites. This assignment is corroborated by the observed energy of the feature, which is in agreement with recent scanning tunneling microscopy studies [15]. It is furthermore observed that the UHB intensity decreases with increasing temperature [Fig. 1(b)], which is consistent with the emergence of a macroscopic coexistence of insulating and conducting domains (corresponding to the different CDW states) up to the critical temperature of 542 K, where the full transition to the normal metallic phase occurs [12].

The distinct response of the UHB becomes evident when the transient energy distribution curves are considered [Fig. 2(a)]. The UHB spectral weight reaches its maximum around $t = 0$ and is lost after 100 fs. This loss is accompanied by ultrafast filling of the gapped region around $E - E_F \approx -0.2 \dots 0.2$ eV. At later delays, only the intensity of the broad continuum remains.

In order to further discuss the temporal evolution of the UHB and separate its dynamics from the underlying continuum, we decomposed both spectral contributions by fitting the energy distribution curves with an exponential background and a Lorentzian line, as shown exemplarily in Fig. 2(b). The fit results are shown in Fig. 2(c) and reveal the ultrafast response of the UHB in contrast to the slower dynamics of the spectral background that exhibits a population decay time of 277 fs. This background is still present at positive delays, when the UHB intensity has disappeared. Correspondingly, the UHB is not populated by secondary excitations, and we conclude that the photoinduced dynamics cannot be described by incoherent scattering processes considering rigid bands. The temporal evolution of the UHB intensity is the fastest response observed in our experiments, and we set its maximum to time zero. Analyzing the dynamics [Fig. 2(c)], we estimate the timescale of doublon-hole recombination to be < 20 fs due to the absence of an exponential decay component within experimental uncertainties (see Supplemental Material for details [22]). This timescale matches approximately the electronic hopping $\hbar/J \approx 14$ fs estimated by dynamic mean field theory [18]. The fast response is furthermore confirmed by the fact

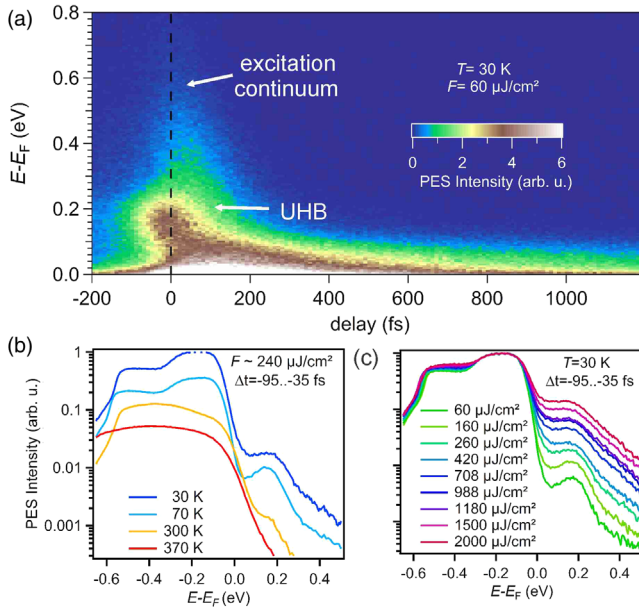


FIG. 1. (a) False-color representation of the time-dependent photoelectron intensity above E_F at 30 K for $F = 60 \mu\text{J}/\text{cm}^2$ in normal emission. Besides an excitation continuum, the upper Hubbard band is observed at $E - E_F \approx 175$ meV in the vicinity of $t = 0$. (b) and (c) show photoemission spectra after excitation for selected T and F , respectively. The spectra were averaged within $\Delta t = -95 \dots -35$ fs. Curves in (b) are offset for better visibility.

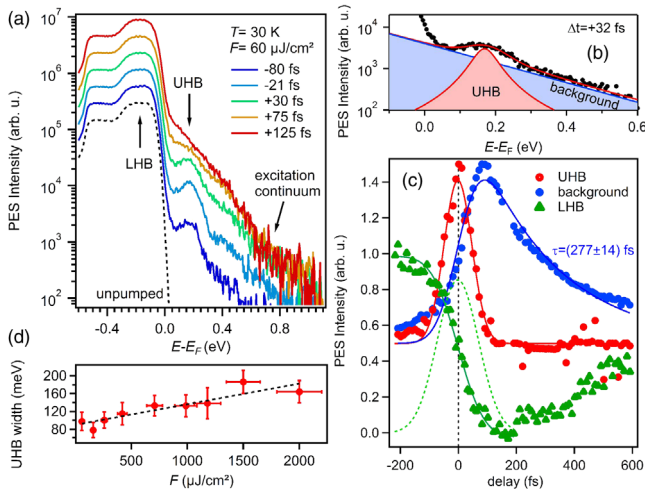


FIG. 2. (a) Transient photoemission spectra obtained for $T = 30$ K and $F = 60 \mu\text{J}/\text{cm}^2$. The curves are offset for better visibility. (b) Exemplary fit to the transient energy distribution curve obtained at $\Delta t = +32$ fs. The superposition of the continuum and the Lorentzian line was convoluted with the instrumental energy resolution function. (c) Temporal evolution of the UHB spectral signature in direct comparison to the underlying continuum and electronic gap, as well as the LHB intensity loss that can be described by an error function (solid green line). The temporal derivative $-(dI/dt)$ of the least mean square fit of the LHB dynamics is shown as a dashed line for comparison with the UHB signal. Curves are rescaled for better visibility. (d) Spectral width of the UHB signature as a function of excitation fluence F .

that the temporal evolution of the UHB coincides with the decrease of the LHB signature that is instantaneously depopulated by the pump pulse [19], and thus can be well described by the temporal integral of the laser pulse cross correlation as shown in Fig. 2(c). This temporal coincidence does not imply a direct optical transition between the LHB and the UHB, whose energy difference of approximately 350 meV in our experiments is largely exceeded by the pump photon energy (1.55 eV). We consider a simultaneous depopulation of the LHB by excitation into higher-lying bands and a population of the UHB due to an excitation from lower-lying states. A corresponding initial state at $E - E_F \approx -1.3$ eV was earlier identified using static ARPES [28,29]. Reducing the pump photon energy to 0.92 eV and 1.04 eV was found to suppress the UHB signature (see Supplemental Material [22]).

For a given excitation fluence, we find that the UHB line profile is independent of t (see Supplemental Material [22]), indicating that the population of the UHB thermalizes on a timescale that cannot be resolved in our experiments. We observe that the energetic width of the UHB signature increases linearly with F [Fig. 2(d)], which excludes the possibility that the photoemission line arises from an unoccupied rigid band populated by the 6 eV probe pulse. We also find that the energy of the UHB line is independent of t (see Supplemental Material [22]), which

indicates that the signature is not related to polaronic excitations discussed in the literature [30]. Our finding rather demonstrates the ultrafast decoupling of electronic and lattice degrees of freedom, since polaron formation would result in an energetic stabilization on phononic timescales. Indeed, the response of the UHB is faster than a quarter period of the highest-frequency phonons in 1T-TaS₂ of 11.9 THz [31], which also implies a decoupling of the doublon dynamics from the periodic lattice distortion associated with CDW formation. We stress that the doublon recombination measured here is related to the dynamics of the occupation, while all-optical experiments probe the dynamics of the joint density of states [32]. In a non-equilibrium situation, there is no simple relation between the two, so both experimental approaches provide complementary information.

Our experimental findings are partly incompatible with the recently proposed energy gap formation based on orbital texturing [16]. Optical excitation of an orbitally ordered system could in principle result in the loss of order due to increased entropy and scattering. The fastest timescale we can imagine is determined by electron-electron scattering which leads to the relaxation dynamics of the excitation continuum; see Figs. 1(a) and 2(a). However, the observed loss of the UHB occurs earlier than that, a fact explained in the present study by local electron-electron correlations. We thus conclude that, while orbital order as well as layer stacking might play a role in electronic band formation, a discussion of the experimentally observed ultrafast electronic response in close vicinity to E_F requires a scenario where electron-electron correlation is considered.

In the following, we discuss a simple theoretical picture based on a purely electronic model and demonstrate how strong interaction is crucial for describing the ultrafast dynamics. We simulate the dynamics of a single-band Hubbard model on a two-dimensional triangular lattice:

$$H = \sum_{i\delta\sigma} J c_{i+\delta,\sigma}^\dagger c_{i,\sigma} + \mu n_i + U \sum_i \left(n_{i\uparrow} - \frac{1}{2} \right) \left(n_{i\downarrow} - \frac{1}{2} \right), \quad (1)$$

where $c_{i\sigma}^\dagger$ denotes the creation operators for a Fermion on lattice site i with spin σ , J is the hopping integral between neighboring sites, μ is the chemical potential, n_i is the number of carriers on site i , and U is the on-site Coulomb repulsion. The electric field of the pump laser $E(t)$ is applied along the (1,1) direction and is incorporated via the Peierls substitution. The parameters were chosen such that, in the absence of an external perturbation [$E(t) = 0$], this Hamiltonian mimics the equilibrium spectral function of single-layer 1T-TaS₂ [15,17] with a bandwidth of $W = 0.36$ eV. Since $U \approx W$, the material is close to the metal-insulator transition, which leads to short recombination times.

The dynamics after optical excitation is modeled by perturbing the system with a Gaussian pulse of the form $E(t) = E_0 \exp[-4.6(t - t_0)^2/t_0^2] \sin[\omega(t - t_0)]$, where the duration of the pulse t_0 is chosen such that it accommodates a single optical cycle. The frequency ω was chosen to be $\omega/J = 8.0$, and the pulse amplitude was $E_0/(Je) = 2.0$. While this pulse frequency generates direct transitions between the LHB and UHB, we have also checked the scenario of photo-doping from lower-lying bands by temporarily coupling an occupied (empty) electron bath to the UHB (LHB). The relaxation dynamics for both protocols is consistent, since it is mainly governed by the excess kinetic energy of the excited doublons. The amplitude of the excitation does not alter the qualitative dynamics as long as one restricts the scenario to the weak excitation regime. To solve the electron dynamics, we use the nonequilibrium dynamical mean field theory [3], which maps a correlated lattice problem onto a self-consistently determined impurity problem [33]. To treat the impurity problem, we use the lowest-order strong coupling expansion, the noncrossing approximation (NCA). To confirm that the resulting dynamics is qualitatively correct, and not sensitive to the details of the band structure, we also employ the one-crossing approximation (OCA) on the Bethe lattice. Realistic gap sizes are obtained for $U = 0.36$ eV in NCA, and $U = 0.43$ eV in OCA.

The transient occupation dynamics is analyzed in terms of the partial Fourier transform of the lesser component of the Green's function $A^<(t, \omega) = \text{Im}[\int_t^{t+t_{\text{max}}} dt' e^{i\omega(t'-t)} G^<(t', t)]$ (occupied density of states). We will first discuss the response of the ideal Mott insulator at half band filling ($n = 1$); see Fig. 3(a). The optical excitation leads to a partial

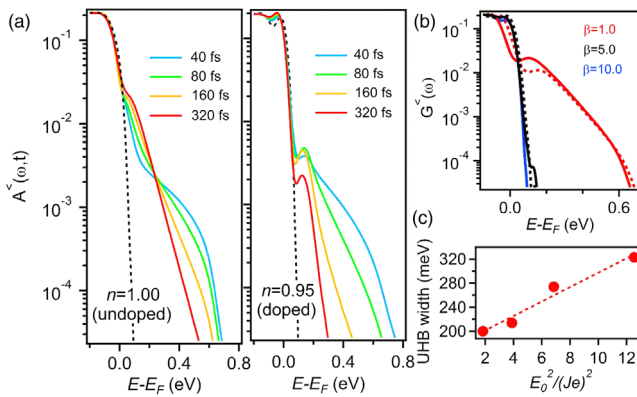


FIG. 3. (a) Time evolution of the occupation function $G^<(\omega, t)$ for a half-filled band ($n = 1$, left panel) and in the hole-doped case ($n = 0.95$, right panel). The dashed lines show the equilibrium situation before excitation. (b) Equilibrium occupation function $G^<(\omega)$ for $n = 0.98$ (solid lines) and $n = 0.95$ (dashed lines) at different temperatures $\beta = (k_B T)^{-1}$, given in units of W ($\beta = 1$ corresponds to a temperature of 32 300 K). (c) Spectral width of the UHB signature at $E - E_F \approx 175$ meV as a function of excitation density E_0^2 . The dashed line indicates a linear dependence.

occupation of the UHB that relaxes within the band and results in a slow population buildup at the lower edge. This prediction of a monotonically increasing UHB population is inconsistent with the experimental observation. It is, however, in agreement with previous studies [34], which show that the thermalization in an isolated small-gap insulator can lead to an increase in double occupation on the timescale of a few inverse hoppings. We note that in contrast to the previous theoretical interpretations [17,18], but in agreement with the experimental data (and recent arguments based on high-temperature expansions [35]), our simulations do not predict a substantial gap filling after photoexcitation.

A more realistic description is obtained if one considers an effectively hole-doped system $1T\text{-Ta}_{(1-x)}\text{S}_2$. Taking into account the indications reported in the Supplemental Material [22], we estimate that the effective filling of the subband straddling E_F can range from half filled ($x = 0$, $n = 1$) to almost empty ($x = 0.03$, $n = 0.17$). To discuss the general influence on the UHB dynamics, we assume a small doping level of $n = 0.95$ [Fig. 3(b)]. In contrast to the half-filled case, the occupation function in the doped case shows a transient increase of the doublon spectral weight, which quickly vanishes. This evolution is in qualitative agreement with the experimental finding.

In agreement with previous works [34,36], the Hubbard band in the small-gap regime thermalizes on the timescale of several inverse hoppings, which we confirmed by checking that the fluctuation-dissipation theorem is fulfilled. Therefore, we can compare the results in the long-time limit with the thermal states at elevated temperatures; see Fig. 3(b). In the half-filled case, the UHB of this small-gap system is always substantially occupied due to the finite overlap of the high-temperature Fermi-Dirac distribution function with the UHB. In the doped case, the Fermi-Dirac distribution is shifted to lower energies, and the overlap with the UHB is exponentially suppressed. In such a situation, a significant population in the UHB can only be achieved at extremely high electron temperatures. This also explains the experimental requirement of low excitation densities to observe the ultrafast reduction of the UHB population and is reflected in the experimental finding that the spectral width of the UHB increases linearly with excitation fluence [Fig. 2(d)], which is also reproduced in the calculation [Fig. 3(c)]. We note that even though electron-phonon coupling is important in $1T\text{-TaS}_2$, we can neglect the phonon dynamics on electronic timescales. In any event, the effect of electron-phonon interactions, as well as short-ranged spin excitations, would be to speed up the relaxation and thermalization [37,38]. This likely explains the faster dynamics in the experiment, compared to the simulations which neglect this physics.

In summary, we identified in a combined experimental and theoretical study the double electron population of cluster sites in $1T\text{-TaS}_2$ and estimated their relaxation time

to be on the order of the electronic hopping \hbar/J . Essential was the time domain approach, which facilitated the detection of doublons before further excitations like secondary electrons or phonons set in. We emphasize the importance of static and photoexcited holes, which enable the ultrafast relaxation on hopping timescales. Our results suggest a tunability of femtosecond dynamics in the vicinity of the Fermi level, which has potential impact for high-frequency applications. More generally, the identification of nonequilibrium signatures of strong electron correlations has led to an improved microscopic understanding of complex materials with competing interactions.

We acknowledge financial support by the Deutsche Forschungsgemeinschaft through SFB 616 (project B08), SPP 1458, SFB 1242 (project B01) and FOR1700 and from ERC Starting Grant No. 278023 and Consolidator Grant No. 724103. L. S. acknowledges the Alexander von Humboldt Foundation. We also thank R. Schützhold and S. Biermann for fruitful discussions. Parts of this research were carried out at the light source PETRA III at DESY, a member of the Helmholtz Association. We thank S. Rohlf and the staff of beamline P04 for experimental support.

*manuel.ligges@uni-due.de

- [1] E. Dagotto, *Science* **309**, 257 (2005).
- [2] C. Giannetti, M. Capone, D. Fausti, M. Fabrizio, F. Parmigiani, and D. Mihailovic, *Adv. Phys.* **65**, 58 (2016).
- [3] H. Aoki, N. Tsuji, M. Eckstein, T. Oka, and P. Werner, *Rev. Mod. Phys.* **86**, 779 (2014).
- [4] M. Eckstein and P. Werner, *Phys. Rev. Lett.* **110**, 126401 (2013).
- [5] D. Golež, J. Bonca, L. Vidmar, and S. A. Trugman, *Phys. Rev. Lett.* **109**, 236402 (2012).
- [6] P. Werner and M. Eckstein, *Europhys. Lett.* **109**, 37002 (2015).
- [7] D. Golež, J. Bonca, M. Mierzejewski, and L. Vidmar, *Phys. Rev. B* **89**, 165118 (2014).
- [8] J. Kogoj, Z. Lenarcic, D. Golež, M. Mierzejewski, P. Prelovsek, and J. Bonca, *Phys. Rev. B* **90**, 125104 (2014).
- [9] M. Eckstein and P. Werner, *Phys. Rev. Lett.* **113**, 076405 (2014).
- [10] D. Golež, M. Eckstein, and P. Werner, *Phys. Rev. B* **92**, 195123 (2015).
- [11] J. A. Wilson, F. J. DiSalvo, and S. Mahajan, *Adv. Phys.* **24**, 117 (1975).
- [12] B. Sipos, A. F. Kusmartseva, A. Akrap, H. Berger, L. Forro, and E. Tutis, *Nat. Mater.* **7**, 960 (2008).
- [13] L. Stojchevska, I. Vaskivsky, T. Mertelj, D. Svetin, S. Brazovskii, and D. Mihailovic, *Science* **344**, 177 (2014).
- [14] M. Klanjšek, A. Zorko, R. Žitko, J. Mravlje, Z. Jagličič, P. K. Biswas, P. Prelovšek, D. Mihailovic, and D. Arčon, *Nat. Phys.* **13**, 1130 (2017).
- [15] D. Cho, S. Cheom, K.-S. Kim, S.-H. Lee, Y.-H. Cho, S.-W. Cheong, and H. W. Yeom, *Nat. Commun.* **7**, 10453 (2015).
- [16] T. Ritschel, J. Trinckauf, K. Koepernik, B. Buchner, M. v. Zimmermann, H. Berger, Y. I. Joe, P. Abbamonte, and J. Geck, *Nat. Phys.* **11**, 328 (2015).
- [17] L. Perfetti, P. A. Loukakos, M. Lisowski, U. Bovensiepen, H. Berger, S. Biermann, P. S. Cornaglia, A. Georges, and M. Wolf, *Phys. Rev. Lett.* **97**, 067402 (2006).
- [18] L. Perfetti, P. A. Loukakos, M. Lisowski, U. Bovensiepen, M. Wolf, H. Berger, S. Biermann, and A. Georges, *New J. Phys.* **10**, 053019 (2008).
- [19] J. C. Petersen *et al.*, *Phys. Rev. Lett.* **107**, 177402 (2011).
- [20] S. Hellmann *et al.*, *Nat. Commun.* **3**, 1069 (2012).
- [21] T. Endo, S. Nakao, W. Yamaguchi, T. Hasegawa, and K. Kitazawa, *Solid State Commun.* **116**, 47 (2000).
- [22] See Supplemental Material at <http://link.aps.org/supplemental/10.1103/PhysRevLett.120.166401> for additional data and details on sample growth and characterization.
- [23] S. Hellmann *et al.*, *Phys. Rev. Lett.* **105**, 187401 (2010).
- [24] This estimation is based on the optical properties reported in Ref. [25] and a geometrical site density of $n = 7 \times 10^{13} \text{ cm}^{-2}$ [26].
- [25] A. R. Beal, H. P. Hughes, and W. Liang, *J. Phys. C* **8**, 4236 (1975).
- [26] A. Yamamoto, *Phys. Rev. B* **27**, 7823 (1983).
- [27] M. Bauer, A. Marienfeld, and M. Aeschlimann, *Prog. Surf. Sci.* **90**, 319 (2015).
- [28] N. Smith, S. Kevan, and F. DiSalvo, *J. Phys. C* **18**, 3175 (1985).
- [29] M. Arita, H. Negishi, K. Shimada, F. Xu, A. Ino, Y. Takeda, K. Yamazako, A. Kimuar, S. Qiao, S. Negishi, M. Sasaki, H. Namatame, and M. Taniguchi, *Physica (Amsterdam)* **351B**, 265 (2004).
- [30] N. Dean, J. C. Petersen, D. Fausti, R. I. Tobey, S. Kaiser, L. V. Gasparov, H. Berger, and A. Cavalleri, *Phys. Rev. Lett.* **106**, 016401 (2011).
- [31] L. V. Gasparov, K. G. Brown, A. C. Wint, D. B. Tanner, H. Berger, G. Margaritondo, R. Gaál, and L. Forró, *Phys. Rev. B* **66**, 094301 (2002).
- [32] A. Mann, E. Baldini, A. Odeh, A. Magrez, H. Berger, and F. Carbone, *Phys. Rev. B* **94**, 115122 (2016).
- [33] A. Georges, G. Kotliar, W. Krauth, and M. J. Rozenberg, *Rev. Mod. Phys.* **68**, 13 (1996).
- [34] P. Werner, K. Held, and M. Eckstein, *Phys. Rev. B* **90**, 235102 (2014).
- [35] E. Perepelitsky, A. Galatas, J. Mravlje, R. Žitko, E. Khatami, B. Shastri, and A. Georges, [arXiv:1608.01600](https://arxiv.org/abs/1608.01600).
- [36] M. Eckstein and P. Werner, *Phys. Rev. B* **84**, 035122 (2011).
- [37] Z. Lenarčič and P. Prelovšek, *Phys. Rev. Lett.* **111**, 016401 (2013).
- [38] Z. Lenarčič and P. Prelovšek, *Phys. Rev. B* **90**, 235136 (2014).